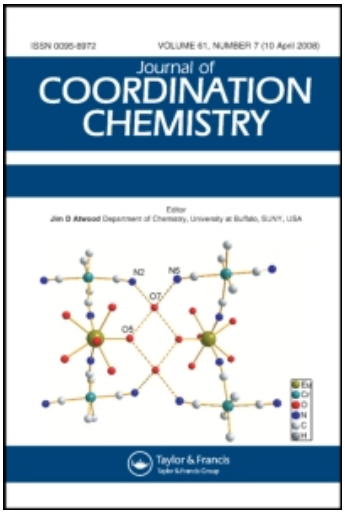

Journal of Coordination Chemistry
Publication details, including instructions for authors and subscription information:
http://www.informaworld.com/smpp/title~content=t713455674

Kinetics of Gallium Removal from Transferrin and Thermodynamics of Gallium-Binding by Sulfonated Tricatechol Ligands

Lawrence D. Loomis[ab]; Kenneth N. Raymond[b]
[a] Department of Chemistry, University of California, Berkeley, CA, USA [b] Department of Immunology, Walter Reed Army Medical Center, Washington, DC, USA

To cite this Article Loomis, Lawrence D. and Raymond, Kenneth N.(1991) 'Kinetics of Gallium Removal from Transferrin and Thermodynamics of Gallium-Binding by Sulfonated Tricatechol Ligands', Journal of Coordination Chemistry, 23: 1, 361 — 387
To link to this Article: DOI: 10.1080/00958979109408265
URL: http://dx.doi.org/10.1080/00958979109408265

J. Coord. Chem. 1991, Vol. 23. pp. 361–387
Reprints available directly from the publisher
Photocopying permitted by license only

KINETICS OF GALLIUM REMOVAL FROM TRANSFERRIN AND THERMODYNAMICS OF GALLIUM-BINDING BY SULFONATED TRICATECHOL LIGANDS

LAWRENCE D. LOOMIS* and KENNETH N. RAYMOND†

Department of Chemistry, University of California, Berkeley, CA 94720, U.S.A.

(Received August 8, 1990)

The thermodynamics of complexation of gallium by tricatechol ligand analogues of enterobactin and the kinetics of gallium removal from human serum transferrin (Tf) by one of those ligands have been studied by UV spectrophotometry. The ligands are a sulfonated monomeric catechoylamide, DMBS (*N,N*-dimethyl-2,3-dihydroxy-5-sulfonatobenzamide), and four sulfonated triscatechoylamides, MECAMS (1,3,5-*N,N',N''*-tris(5-sulfonato-2,3-dihydroxybenzoyl)-triaminomethylbenzene), Me_3MECAMS (*N,N',N''*-trimethyl-MECAMS), 3,4-LICAMS (*N,N',N''*-tris(5-sulfonato-2,3-dihydroxybenzoyl)-1,5,10-triazadecane), and (DiP)LICAMS (*N,N''*-diisopropyl-LICAMS). The individual *ortho*hydroxyl protonation constants are 7.15 (DMBS), and (average values for the three protons of the tricatechols) 7.09 (MECAMS), 7.01 (LICAMS), 7.62 (Me_3MECAMS), and 7.75 ((DiP(LICAMS), in good agreement with average values obtained potentiometrically. The overall formation constants for binding of Ga^{3+} by these ligands are $\beta_{113} = 41.9$ for DMBS, $\beta_{110} = 41.1$ for LICAMS, 36.6 for (DiP)-LICAMS, and 39.1 for Me_3MECAMS. Gallium is removed from the two metal binding sites of Ga_2Tf in a process by 3,4-LICAMS that is first order in both Tf and ligand at different rates ($277\ M^{-1}min^{-1}$ and $17\ M^{-1}\ min^{-1}$). These are 12 and 3.4 times the corresponding rates of iron removal from Fe_2Tf. The dissociation pathways of the gallium-ligand complexes upon protonation of the ligands were probed by whole spectrum analysis with the non-linear least-squares program REFSPEC. For all three triscatechoylamide complexes, protonation occurs in sequential one-proton reactions wth logK MLH_n (n = 1, 2, 3) equal to 5.93, 5.00, 2.4 for MECAMS: 5.8, 5.7, 3.0 for 3,4-LICAMS; 6.81, 6.34, 3.0 for Me_3MECAMS; 6.34, 6.33, 4.3 for (DiP)LICAMS. First- and second-derivative spectra show that for complexes of trimeric ligands the last two protonations result in a complex with a completely dissociated catecholate arm, $Ga(cat)_2$-$catH_2$, similar to the $Ga(DMBS)_2$ complex observed with the monomer. In the linear complexes, the middle ligand arm is detached from the metal first. Addition of a fourth proton resulted in decomposition of the gallium-trimeric ligand complex.

Keywords: Gallium, radiopharmaceuticals, chelating agents, imaging

INTRODUCTION

The radionuclide ^{67}Ga is an important component of the current radiopharmaceutical repertoire.[1] Because Ga^{3+} is similar to Fe^{3+} in charge and ionic radius, in living systems gallium is transported by *metabolic pathways* that are similar in several aspects to those of iron.[2,3] When injected into a test subject as the citrate complex, ^{67}Ga binds rapidly to transferrin, the major iron-binding protein found in mammalian blood;[4–8] in a process mediated by transferrin, the isotope becomes preferentially localized in faster-growing tumor cells and damaged tissues.[9–11] The radionuclide is a gamma emitter and can be used to locate tumors and abcesses by whole-body

* Present address: Department of Immunology, Walter Reed Army Medical Center, Washington, DC 20307, U.S.A. † Author for correspondence.

scanning.[12] Disadvantages to this tumor-imaging process include slow clearance of the radiopharmaceutical from the body,[2,3] and the isotope's relatively long half-life (3.26 days). These factors can lead to an undesirably high radiation dosage to the patient and reduce the efficiency of the imaging process by lowering the target to non-target radioactivity ratio.

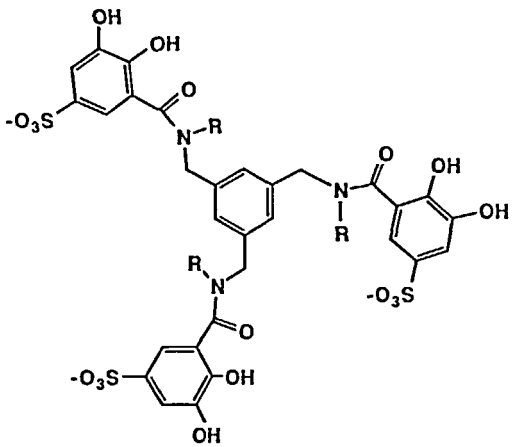

R = H; MECAMS
R = CH_3; Me_3MECAMS

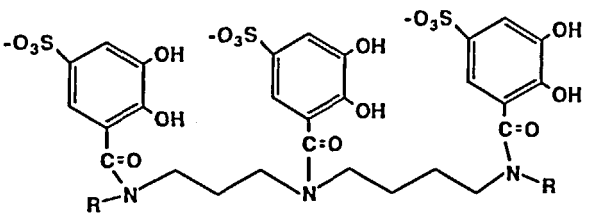

R = H; LICAMS
R = CH-$(CH_3)_2$; (DiP)LICAMS

FIGURE 1 Structures of some synthetic sulfonated catechoylamide (CAMS) ligands. Abbreviations: MECAMS (R = H) = 1,3,5-*N*,*N*′,*N*″-tris(5-sulfonato-2,3-dihydroxybenzoyl)-triaminoethylbenzene; Me_3MECAMS (R = CH_3) = *N*,*N*′,*N*″-trimethyl-1,3,5-*N*,*N*′,*N*″-tris(5-sulfonato-2,3-dihydroxybenzoyl)-triaminomethylbenzene. LICAMS (R′ = H) = *N*,*N*′,*N*″-tris(5-sulfonato-2,3-dihydroxybenzoyl)-1,5,10-triazadecane; (DiP)LICAMS (R′ = –CH–$(CH_3)_2$) = *N*,*N*″-diisopropyl-*N*,*N*′,*N*″-tris(5-sulfonato-2,3-dihydroxybenzoyl)-1,5,10-triazadecane.

Synthesis of a biologically tolerable ligand which removes excess gallium from the blood but not from tumors is a medically important goal. Drugs currently available for this purpose, including desferriferrioxamine B,[13,14] require high doses, and are undesirable because of their relative toxicity and kinetic inability to remove metals

from transferrin.[15] Previous studies on iron coordination chemistry have led to the development of synthetic ligands based on known biological chelators, such as enterobactin and parabactin, which contain the catechoylamide moiety (1,2-dihydroxybenzamide).[16-18] To overcome the limitations of currently available drugs, several of these synthetic catechoylamide derivatives ("CAMS"), Figure 1, have been studied as possible Ga^{3+} complexing agents.[19,20]

Potentiometric titrations of the CAMS-ligands show two regions of deprotonation.[21,22] The first of these regions occurs between pH 5.5 and 9 and corresponds to loss of the three protons on the hydroxyl groups ortho to the carbonyls. The average log values of the *meta* hydroxyl protonation constants of DMBS, MECAMS, and 3,4-LICAMS have been estimated by spectrophotometric titration with analytically determined concentrations of strong base to be greater than 10.[23] The sulfonate groups are strongly acidic and so are fully deprotonated in the solutions studied.

Potentiometric results have shown that these ligands bind both Ga^{3+} and Fe^{3+} very strongly. At physiological pH and above, the hexadentate complexes with gallium have formation constants, log K_f, of the order of 38.[21,22] As the acidity of the medium is increased, the catechol groups protonate and release the metal ion. There are only two buffer regions, from zero to two equivalents of added acid, and between two and six acid equivalents. The ferric complexes of these ligands have also been studied spectrophotometrically, relying on pH-dependent changes in ligand-to-metal charge transfer transitions in the visible region of the spectrum.[24,25]

A fundamental question about the mechanism of metal–CAMS binding process remains. Do the fully formed hexadentate complexes protonate *via* two-proton steps with dissociation of a catechol group at each step or do they protonate by one proton steps, shifting to a salicylate mode of bonding (Figure 2)? Presuming a "salicylate shift," does this happen three consecutive times, before the fourth proton completely dissociates a catechol ring, or in a concerted fashion accompanied by metal–ligand dissociation? Several studies have shown that, in general, the ferric–CAMS systems protonate *via* three successive salicylate shifts.[26,27] For the gallic–CAMS systems, the potentiometric data for the buffer region between zero and two equivalents of added acid can be fitted successfully either with a pair of closely spaced one-proton steps, or a single two-proton step. The relatively featureless titration curve encompassing four to six equivalents of added acid has not yielded to detailed analysis.

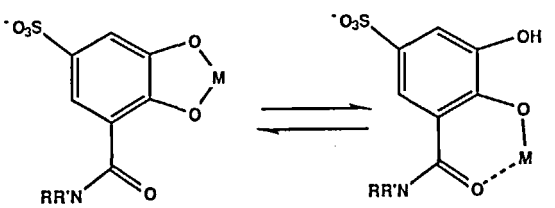

FIGURE 2 Representation of the catecholate (left) and salicylate (right) modes of bonding between a metal and CAMS ligand.

Transferrin binds two metal atoms per protein molecule at similar, but chemically and spectroscopically distinguishable, sites.[4,28-30] Previous studies have shown the kinetics of iron removal from transferrin by these ligands is quantitative and relatively rapid.[31-35] Gallium is bound to the two sites of transferrin under

physiological conditions with conditional formation constants (pH 7.4, 27 mM $NaHCO_3$):[36]

$$K_1^* = [GaTf]/[Ga][Tf] \qquad \log K_1^* = 20.3$$

$$K_2^* = [Ga2Tf]/[Ga][GaTf] \qquad \log K_2^* = 19.3$$

These constants are relatively low with respect to the hydrolysis of gallium und these conditions;[37] approximately 80% loading is possible, with substantially mo binding to the high affinity C terminal site. Comparison of binding constants sho that the CAMS ligands are thermodynamically capable of removing gallium fro transferrin. To be used as gallium removal drugs *in vivo*, they must also be kinetical rapid in doing so. This study for the first time examines the rate of gallium remov from Tf.

Two models have been proposed for the mechanism of iron removal fro transferrin; the schemes, and kinetic models for each of them, have been summarize in detail.[31,32] One of the models proposes that the rate limiting step in metal remov is a protein conformation change.[38] If this is true, then the maximum rate at whic metals can be removed from Tf is a constant, regardless of metal or removal age used. To date experimental tests of this hypothesis have involved changing t ligands that were used to remove iron. It should also be possible to address th proposal by changing the metal removed. However, since the kinetics of binding iron by CAMS ligands is most readily followed spectrophotometrically, this mig seem a barrier for corresponding gallium systems since the Ga(III) complexes ha no visible absorption characteristics. On the other hand, previous thermodynam studies on metal removal from transferrin followed protein spectral changes by U difference spectroscopy.[39] The CAMS ligands absorb strongly in the ultraviol (UV). UV spectra are perturbed upon protonation or metal-binding sufficient to allow determination of thermodynamic constants for the ligands alone an metal–ligand complexes. These ligand-based transitions were studied using derivati spectrophotometric techniques and whole spectrum analysis to verify a scheme f the pH-dependent coordination of gallium by CAMS ligands. In addition, t catechoylamide ligand spectral absorbances were monitored to measure the rates gallium removal from transferrin by 3,4-LICAMS and to see if the biphas behaviour found for iron removal from the native protein also occurs for the gall protein complex.[31,32]

EXPERIMENTAL

Materials

Distilled, deionized water was used to prepare all solutions. Salts and buffers we reagent grade; HEPES buffer (*N*-2-hydroxyethylpiperazine-*N'*-2-ethanesulfonic aci log A = 7.55, Calbiochem) was 50 mM, in the Na^+ form, pH 7.4 at 25°C. Dialys tubing was obtained from Bethesda Research Laboratories and was prepared b boiling in water and stored in 0.1% EDTA. Human serum transferrin (Tf) w obtained from Calbiochem-Behring. Gallium metal (J.T. Baker) was boiled in a 5 mixture of HNO_3 and HCl for several hours, yielding a clear solution of Ga^{3+} i concentrated acid. This was diluted to approximately 0.1 M with distilled, deionize

H_2O, and standardized by direct titration with EDTA in pH 3.8 acetate buffer and 0.1% aqueous pyrocatechol violet indicator; optimal conditions for the standardization employed a final Ga^{3+} concentration of about 0.6 mM.[40] Concentrations obtained were verified by atomic absorption spectroscopy. The syntheses of all ligands used are reported in detail elsewhere.[41-43] The effective molecular weights were obtained by potentiometric titrations, and verified by microanalyses. Analyses were performed by the U.C. Berkeley microanalytical laboratory.

Apparatus

UV spectra were recorded using a Hewlett-Packard 8450A diode array spectrophotometer. Spectra absorbance averaged over multiple wavelengths and derivative spectra ($dA/d\lambda$ and $d^2A/d\lambda^2$) were obtained digitally using built-in algorithms of that spectrometer.[44] Cuvettes were maintained at 25°C using an HP thermostatted temperature controller. Titrations were performed in locally-made, jacketted titration vessels which maintained the solutions at 25°C with a circulating water bath. The $-\log[H^+]$ was monitored using a Corning 130 digital pH meter and combination electrode, calibrated to $[H^+]$ with analytically prepared solutions of acid.

Gallium–Transferrin Preparation

Human serum transferrin was dissolved in water (20 mg cm^{-3}) and dialyzed at 4°C for no less than nine hours *vs* three changes of HEPES buffer containing 1 mM sodium bicarbonate.[32] Protein concentration was calculated using ε (279 nm) = 96,000 1 mol^{-1} cm^{-1}; this value was determined by direct titration with standard iron solutions and is within 5% of previously reported values.[45,46] Gallic transferrin was prepared from apoTf by adding gallium chloride stoichiometric to the calculated number of binding sites, as previously described.[36] No complexing agent was used for delivery of Ga^{3+}. Loading was monitored by UV difference spectroscopy; 80% saturation was obtained using this method, assuming $\Delta\varepsilon$ of 20,000 (242 nm) per gallium bound.[36] Several hours were allowed to reach equilibrium; no spectral changes were observed after approximately one hour. In order to remove nonspecifically bound metals, both apo- and gallic-Tf were dialyzed at 4°C for at least 24 hours against several changes of HEPES buffer which contained 0.1 M sodium perchlorate. The protein solutions were dialyzed *vs* three more changes of HEPES buffer before use.

Spectrophotometric Titrations

Solutions were made up to approximately 0.1 mM in ligand, yielding absorbance values between 0.1 and 1.8 in the near UV region (1 cm path). Ligand solutions were made up to 0.1 M ionic strength using KCl. In order to obtain the lowest possible pH while maintaining ionic strength, the metal–ligand solutions were made up in 0.1 M HCl; the ionic strength was maintained throughout the pH region studied by the sum of hydrogen ion + generated KCl + hydroxide ion. In titrations involving gallium metal, the metal was added last in order to minimize metal hydrolysis. The titrations typically encompassed the pH range from 5 to 10 (ligand alone) or from 1 to 7.5 (metal–ligand). The pH was raised by addition of small aliquots of concentrated KOH; pH changes ranged from 0.070 to 0.250. After each addition of titrant, equilibrium was generally obtained in under five minutes, except at high pH in the

metal–ligand titrations where time periods up to one-half hour were required. Spectra were recorded by transferring an aliquot from the titration vessel to a cuvette which was firmly seated in the spectrophotometer and never moved during the course of the titration (to minimize baseline shifts). Volume corrections were applied for added titrant (generally on the order of 0.5% dilution). A typical data set included 40 to 70 points.

Kinetic Studies

Kinetic studies of gallium removal from gallic-Tf using from 5- to 30-fold excess LICAMS were performed, monitoring changes in the UV difference spectra. Protein concentrations were from 35 to 55 μM. A background was initially measured with apo-Tf and ligand in the desired concentrations in both sample and reference cells. The solution in the sample cell was carefully replaced with the gallic-Tf. Ligand was added to the sample cuvette, the solution was mixed rapidly, and difference spectra recorded as a function of time.

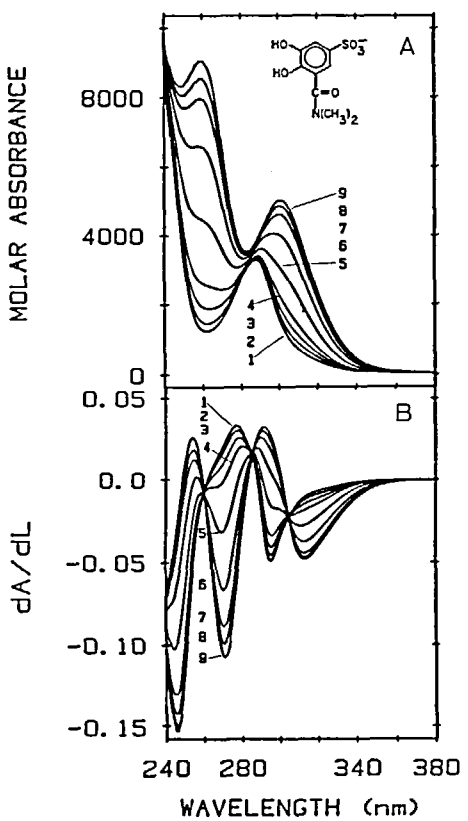

FIGURE 3 Titration of 0.26 mM DMBS (*N,N*-dimethyl-2,3-dihydroxy-5-sulfonatobenzamide, see insert). Spectra have been corrected for dilution and random baseline shifts. For better contrast, every fourth spectrum is shown: 1) pH 4.95, 2) 5.46, 3) 6.03, 4) 6.43, 5) 6.98, 6) 7.49, 7) 7.97, 8) 8.37, 9) 9.03. A) Absorbance spectra. B) First derivative spectra. Isosbestic points are observed at 260, 285, and 305.

RESULTS

Titrations

DMBS ligand only

Spectral changes in the titration of DMBS alone were observed with changes in pH above 4.0 (Figure 3). The low pH absorbance at $\lambda_{(max)} = 287$ nm ($\varepsilon = 3200\ M^{-1}\ cm^{-1}$) shifted to lower energy upon deprotonation of the ligand, while becoming more intense --$\lambda_{max} = 301$ nm ($\varepsilon = 5000$) at pH 9. In addition, an intense peak grew in at 260 nm (9000). These are assigned to transitions of the catechol ligand that are aromatic π to π^* in character.[47]

In order to determine whether these spectral changes could be used to obtain thermodynamic information about the system, the method of Schwarzenbach was applied first, (*1*) and (*2*).[48]

$$A = (\varepsilon_2)c_T + \frac{(A_0 - A)}{[H^*]^N} = K_H \qquad (1)$$

$$\frac{dA}{d\lambda} = \left(\frac{d\varepsilon_2}{d\lambda}\right)c_T + \frac{\frac{dA_o}{d\lambda} - \frac{dA}{d\lambda}}{[H^+]^N} = K_H \qquad (2)$$

Here, A = absorbance, A_0 = initial absorbance, λ = wavelength, K_H = dissociation constant, N = proton stoichiometry, H^+ = hydrogen ion concentration, c_T = total concentration, and ε_2 = molar extinction coefficient (for the less protonated species). This method requires that there be only two absorbing species in solution. The presence of an isosbestic point is generally a good indication that there are only two absorbing species; in the DMBS titration, however, no crossovers were observed even though only two species were anticipated from the following equilibrium.

$$H_2DMBS^- = HDMBS^{2-} + H^+K_1$$

However, the lack of an isosbestic point in the absorbance spectra does not preclude the existence of only two species, but may be the result of spectra for which the molar extinction values never cross. The derivative spectra vary much more and routinely have several crossover points of $d\varepsilon/d\lambda$ for two different species. In this case, isosbestic points were noted in the derivative spectra $dA/d\lambda$ (Figure 3b). The method of Schwarzenbach is applicable to derivative spectra as well as unmodified absorbance data, (*1*), since only ε and A are functions of λ (see also Discussion). A modified absorbance function was used in the Schwarzenbach calculations to increase the ratio of signal to noise.[49-51] The equation was linear only when one-proton stoichiometry was assumed, Figure 4; the calculated log A is 7.13.

The data set was also analyzed using REFSPEC, a program for factor analysis and refinement of thermodynamic constants from spectral data.[49,50] The first step in the refinement process involves the calculation of spectra components which are common to all of the spectra. The number of components found generally will be equal to the number of absorbing species in solution. After selecting components, a suitable model must be chosen for the reactions involved. The program refines the thermo-

dynamic constants required for that model by minimizing the difference between the observed (Y_{obs}) and calculated (Y_{calc}) coefficients of each component required to describe the spectrum at each pH. Finally, species distributions and molar absorbance spectra for each species are calculated, so that the refined theoretical model can be verified against observable properties.

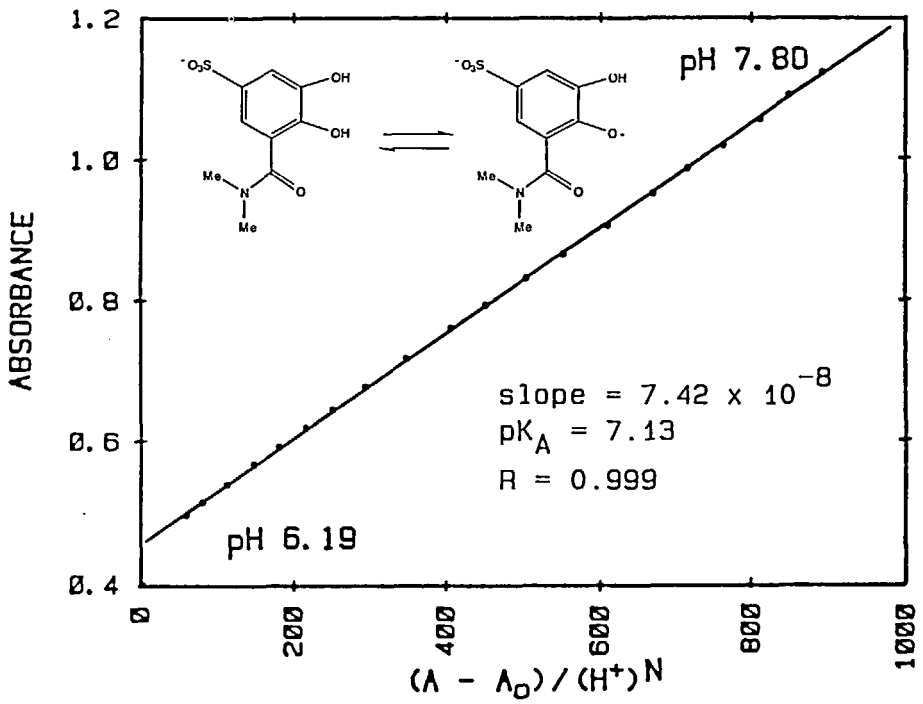

FIGURE 4 Schwarzenbach plot of the data from the isosbestic region of the DMBS titration. The wavelengths used in absorbance calculation were [Ave(λ 295 to λ 305)–Ave(λ 390 to 400)] in order to minimize small fluctuations in absorbance and baseline shifts.

Only two components were found in the spectra for the titration, implying the existence of only two absorbing species (Figure S1).[52] The protonation constant of the *meta* OH is 12.3 and so does not influence the spectra below about pH 10.5.[27] The two component model (*2*) yielded a logK of 7.15. The agreement in the plots of observed *vs* calculated component coefficients was excellent and the model yielded a plausible two-component species distribution (Figures S2 and S3).[52] The extinction coefficient spectra calculated from the data (Figure S4)[52] are in close agreement with the low and high pH spectra observed in the titration. The extinction coefficients for the various species are collected in Table I.

Gallium–DMBS

The titration of a 1:3 stoichiometry of Ga to DMBS from pH 1.2 to 8.7 are shown in Figure S5.[52] The low pH spectrum is identical to that of the fully protonated ligand as determined from the factor analysis; at high pH, λ max = 307 (ε approx. 20,000).

TABLE I

Spectral properties of DMBS, triscatecholate ligands, and complexes with gallium as a function of protonation state.

	Spectral Properties: λ_{max} (ε)									
	Ligand Alone						Ga Complex			
Ligand[a]	LH_6	LH_5	LH_4	LH_3	LH_2	L^b	MLH_3	MLH_2	MLH	ML
3,4-LICAMS	292	322	327	322	316	339	Broad	328	Broad	329
	(6,000)	(6,700)	(8,700)	(10,000)	(12,000)	(12,000)		(8,700)		(10,600)
DiP-LICAMS	287	288	293	300	301		291	303	303	307
	(8,200)	(8,800)	(10,400)	(13,800)	(14,000)		(10,200)	(12,400)	(15,800)	(21,000)
MECAMS	310	319	328	329		347	326	327	333	334
	(8,000)	(9,000)	(13,000)	(14,000)		(15,000)	(10,600)	(11,000)	(13,900)	(15,900)
Me_3MECAMS	288	290	296	301			299	304	305	312
	(9,300)	(10,600)	(12,400)	(15,400)			(9,300)	(10,400)	(11,200)	(16,400)
DMBS[c]	288			301		313		305		307
	(3,300)			(5,000)		(6,400)		(12,200)		(20,100)

[a] Note: see Figure 1 for structures. [b] Reference 23. [c] Values for DMBS are for LH_2, LH^-, and L^{2-} (ligand) and for ML_2 and ML_3 (Ga complex). Not adjusted for the different number of chromophores per molecule; for ML, ε = 6,900 at 302 nm.

Three buffer regions were clearly resolved, corresponding to pH regimes in whic primarily the mono-, bis- and tris-complexes dominated. In addition to the ligan protonation (*2*), the model for this system included hydrolysis and complexatic equilibria, (*3*), (*4*).

$$Ga^{3+} \xleftrightarrow{OH^-} Ga(OH)^{2+} \xleftrightarrow{OH^-} Ga(OH)^{2+} \xleftrightarrow{OH^-} Ga(OH)3 \xleftrightarrow{OH^-} Ga(OH)_4^- \quad (3$$

$$Ga^{3+} \underset{\beta 110}{\overset{DMBS^{3-}}{\longleftrightarrow}} Ga(DMBS) \underset{\beta 120}{\overset{DMBS^{3-}}{\longleftrightarrow}} Ga(DMBS)_2^{3-} \underset{\beta 130}{\overset{DMBS^{3-}}{\longleftrightarrow}} Ga(DMBS)_3^{6-} \quad (4$$

The ligand protonation constant was fixed at the value determined from the ligan titration. The metal hydrolysis constants were fixed at the reported values[53] (th hydrolysis products were assumed to have no effect on the absorbance spectrum). A the formation constants were refined, using a five component model (the absorbin species in the model included the protonated and mono-deprotonated ligand and th three complexes of the ligand with gallium). The values for the formation constan obtained using this model ($\beta_{in0} = [ML_n]/[ML_{n-1}][L]$) are compiled in Table II. Th species distribution and extinction coefficient spectra obtained with these values ar shown in Figure 5. The maxima in the spectra, Table I, agreed well with the spectr observed in the three distinct buffer regions. Other trial models which incorporate hydrolysis products of the tris complex, such as ML_3OH, or which allowed dime formation, such as M_2L_2, failed to refine.

Triscatecholate ligands

The spectra obtained in the titrations of MECAMS and Me_3MECAMS are shown i Figure S6.[52] The latter were similar to the spectra observed for (DiP)LICAMS. Th fourth ligand, 3,4-LICAMS, displayed substantially different spectroscopic proper ties; it will be considered separately at the end of this section. For all titrations spectral changes were observed only between about pH 5 and 10. Below pH 5, th fully protonated ligand was the only absorbing species, and the triply *ortho* deprotonated species predominated above pH 10. The low pH band grew in intensit and shifted to lower energy as pH was increased. This is assigned to a carbony non-bonding to aromatic π electronic transition (consistent with the great effect tha *N*-alkylation has on the spectra).

Analyses of these systems were complicated by overlapping equilibria, (*5*)

$$LH_6 \underset{K_6}{\longleftrightarrow} LH_5 + H + \underset{K_5}{\longleftrightarrow} LH_4 + H + \underset{K_4}{\longleftrightarrow} LH_3 + H + \quad (5$$

Since the three protonation constants for these systems occurred within approxi- mately two pH units, and some contribution from LH_2 was also possible at high pH, the spectra were analyzed using REFSPEC. In the cases of MECAMS and Me_3MECAMS, four components were found; five were found for 3,4-LICAMS and its derivative. In the former, the model shown in (*6*) was used; in the latter, LH_2 was included. The values for K_3, where included, were fixed to values known or estimated from other data.[23,42] All four systems refined well; a representative fit is shown in Figure S7.[52] The equilibrium constants obtained are summarized in Table

TABLE II
Thermodynamic constants obtained for DMBS and triscatecholate ligands as gallium complexes.

	Ligand Protonation (log values)			Average Constants		Ga Complex[a]			
Ligand	(K_6)	(K_5)	(K_4)	Ortho	Meta[b]	pK_{MLH}	pK_{MLH_2}	pK_{MLH_3}	β_{110}
3,4-LICAMS	5.97[c]	6.99	8.07	7.01	12.1	5.8[c]	5.7	3.0	41.1
	(6.11)[d]	(7.07)	(8.28)	(7.15)		[e]	(10.2)		(38)
DiP-LICAMS	7.13	7.79	8.34	7.75		6.34	6.33	4.3	36.6
	(7.13)	(7.78)	(8.50)	(7.80)			(12.1)		(36)
MECAMS[f]	6.50	7.00	7.77	7.09	11.9	5.93	5.00	2.4	41.0
	(5.88)	(6.44)	(7.26)	(6.53)		(5.7)	(4.9)		(38)
Me_3MECAMS	6.79	7.52	8.56	7.62		6.81	6.34	3.0	39.1
	(6.72)	(7.57)	(8.52)	(7.60)		(7.2)	(5.8)	(3.1)	
DMBS				7.15	12.3				41.9[g]
				(7.26)					(38)

Note: See Figure 1 for structures. [a] The overall formation constant was refined for all systems except Ga-MECAMS in which it was fixed at the same value as obtained for LICAMS; the MECAMS system diverged for all models tested in which β_{110} was allowed to vary. [b] All values for *meta* deprotonations, Reference 23. [c] Spectrally obtained values, this work. [d] Potentiometrically obtained values, References 25 and 40. [e] Values in parentheses were obtained potentiometrically, References 21 and 22. The e.s.d.'s for the spectrally obtained values are 0.02 for the two two pK_A's and 0.05 for pK_3. [f] The largest differences in average value between the two methods are seen for the non-alkylated ligands. These are attributed to the use of new values for the high pH protonations which were obtained since the potentiometric results (Reference 23). [g] β_{130}, β_{110} = 18.1; 15.5, Reference 21; β_{120} = 33.0; 29, Reference 21. are used as reference data.

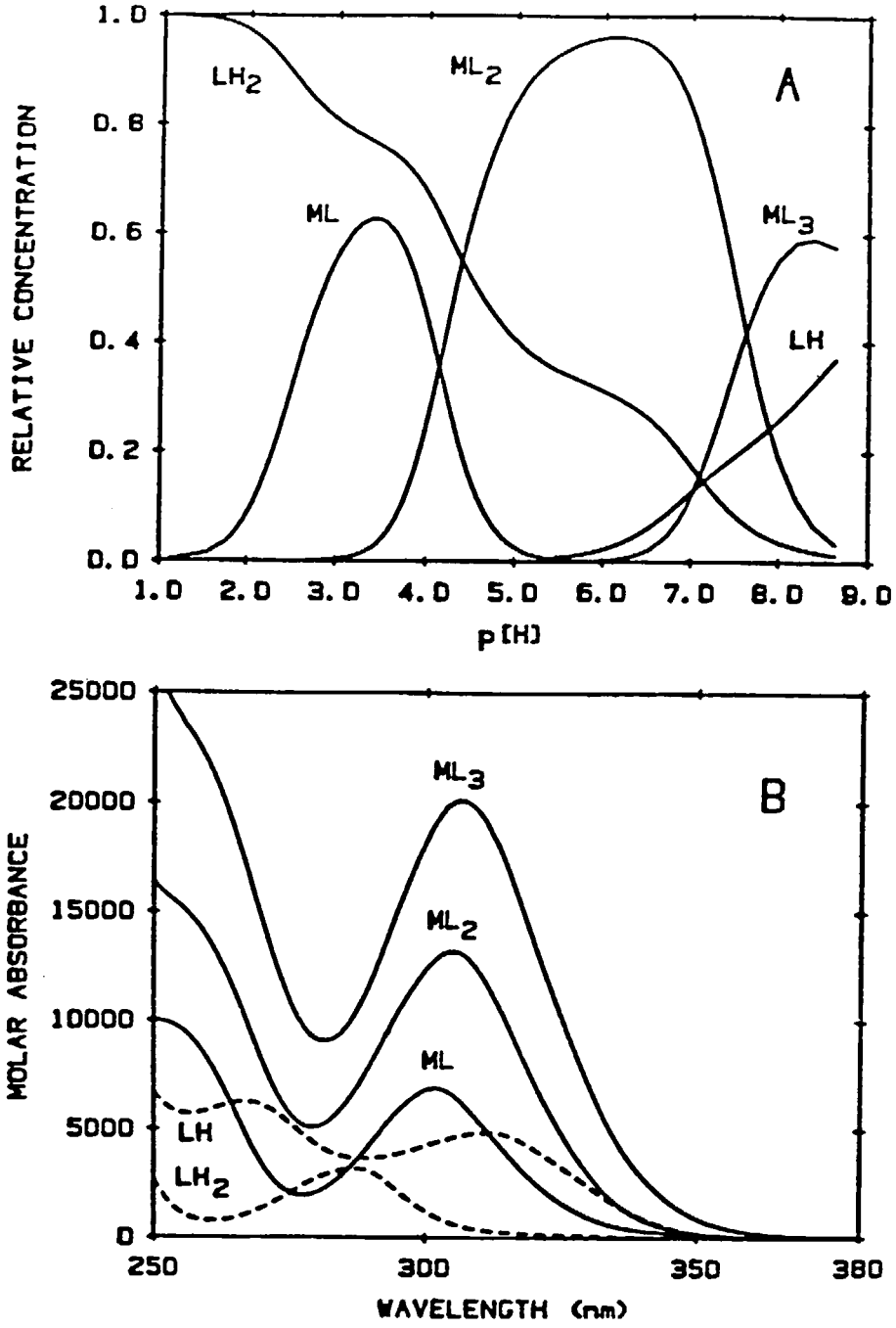

FIGURE 5 A) Species distribution calculated for gallium–DMBS, as a function of pH. Metal complexes are normalized to total metal concentration, species not containing metal are normalized to total ligand concentration. B) Extinction coefficient spectra calculated for the five species in the gallium-DMBS titration.

II. The values obtained previously from potentiometric titration are also included in this table. The species distributions calculated using the constants obtained, illustrated in Figure 6 for MECAMS, show the high degree of overlapping equilibria which makes non-linear least-squares analysis necessary here.

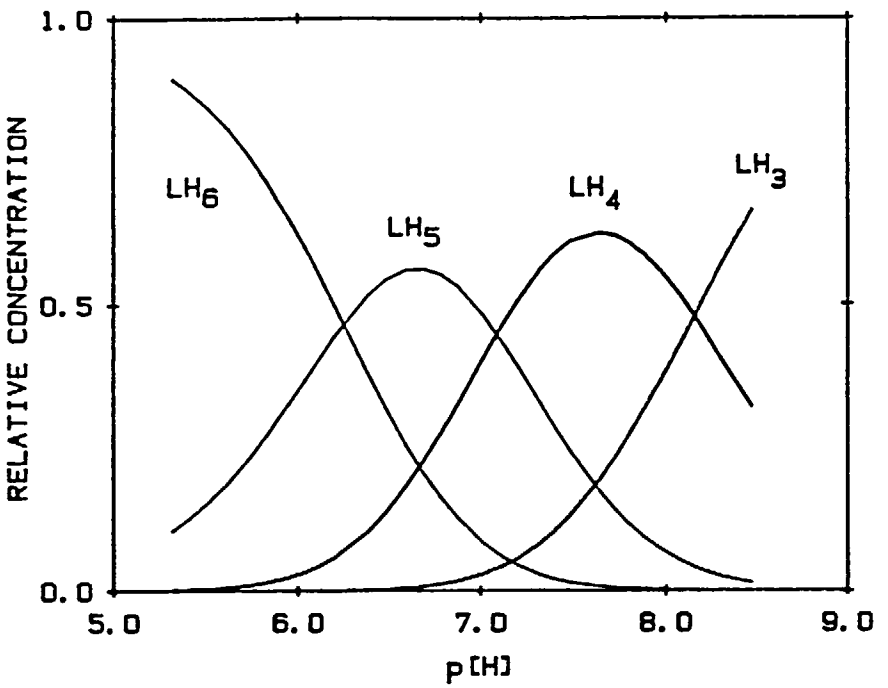

FIGURE 6 The pH-dependent distribution of the four species found in the MECAMS system, normalized to total ligand concentration.

An important result of these refinements is the resolution of the absorption spectra of the individual species in solution. The calculated spectra for MECAMS and its methyl derivative are compared in Figure 7; the (DiP)LICAMS spectra are quite similar to those of Me_3MECAMS. The 3,4-LICAMS spectra are very different and will be considered separately. No crossovers are observed in the spectra of either of the alkylated derivatives, as anticipated from the titration data. The extinction coefficient spectra of MECAMS display isosbestic points which apply to all four absorbing species. The spectral properties of the partially protonated species are summarized in Table I.

The observed and calculated spectra for 3,4-LICAMS are shown in Figure 8. The transition of interest is greatly broadened in comparison to that of the other ligands; the spectra are suggestive of two or more partially separated peaks. The second derivative ($d^2A/d\lambda^2$) will often separate spectra which overlap, showing a minimum at the absorbance maximum of each component.[54-56] The derivative spectra of 3,4-LICAMS at pH 7.5, where LH_4 is the dominant species in solution, and at high pH, where LH_3 predominates, are shown in Figure 8. The second derivative (dashed line) does indeed indicate that there are multiple underlying peaks. The LH_3 species has

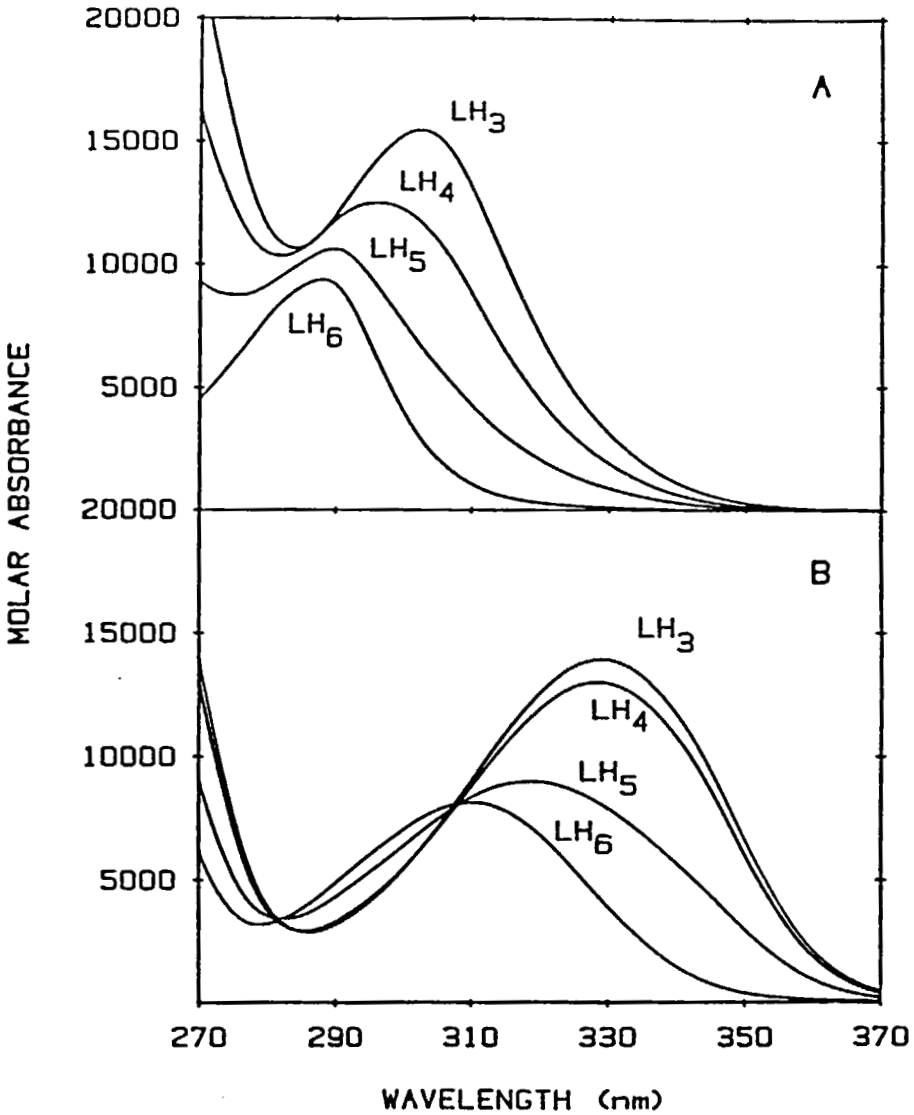

FIGURE 7 Extinction coefficient spectra for A) Me_3MECAMS and B) MECAMS. The spectra of (DiP)LICAMS resemble those of Me_3MECAMS.

two or three bands. One sharp minimum appears at 304 nm, and a broader one (possibly a doublet) is centered at 335 nm. The low pH spectrum lacks the peak at 304 nm.

Gallium–CAMS

The spectrophotometric titrations of 1:1 complexes of gallium with MECAMS and Me_3MECAMS—which is similar to (DiP-LICAMS)—are shown in Figure S8.[52] The

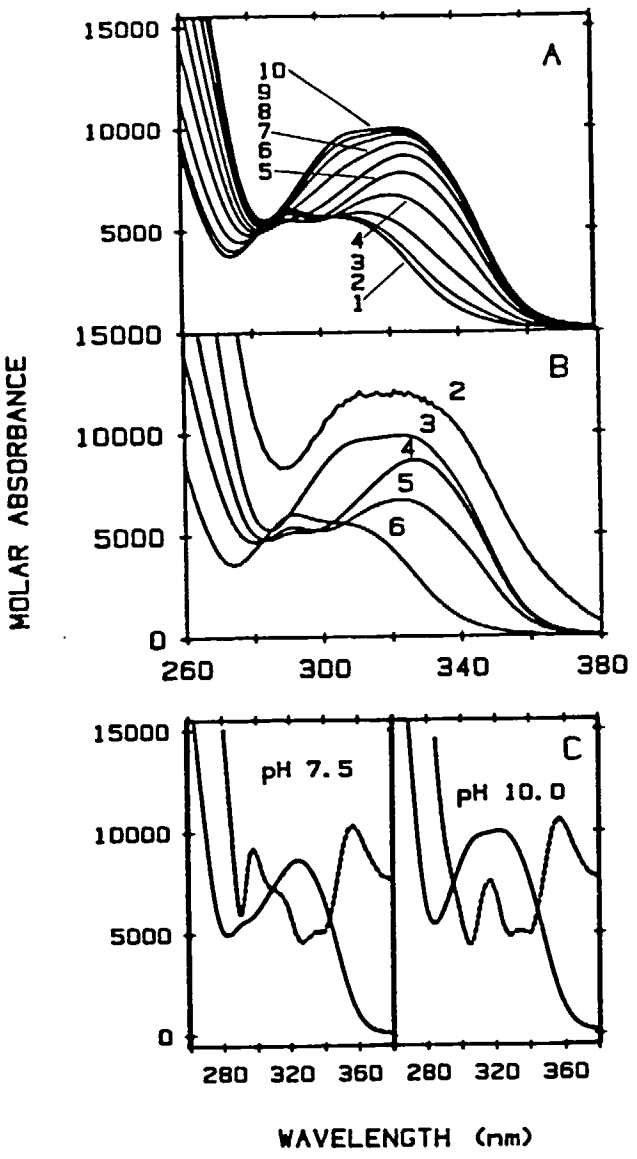

FIGURE 8 Spectroscopic properties of LICAMS. A) Titration of 94.0 μM ligand, every 7th spectrum shown; successive spectra are separated by 0.5 pH units, 1) 5.01, 10) 10.01. B) Extinction coefficient spectra calculated for the four components used in the refinement. The numbers, N, represent the protonation state of the ligand, LH_N; *i.e.*, "3" is the triply protonated species, LH_3, and "6" is the fully protonated form. C) Absorbance spectra (-----) and first derivative spectra (- - - - -) at pH 7.5 (left-hand side) and pH 10.0 (right-hand side) where H_4LICAMS and H_3LICAMS, respectively, predominate in solution.

spectra at the lowest pH values were identical to those of fully protonated ligand determined from factor analysis. At high pH, the peaks shifted to lower energy and increased in intensity. Compared to the ligands, however, the spectral changes all occurred at much lower pH, in accordance with potentiometric studies. Two buffer regions were clearly observed—the spectra with absorptions at higher energy correspond to between zero and four equivalents of added base, and the spectra with lower energy absorptions correspond to the last two equivalents. These changes indicate that there is a direct reaction between the free ligand to that fully complexing the metal, losing six protons in the process.

Initial analysis of the deprotonation stoichiometry was by the method of Schwarzenbach. As in the earlier example, no isosbestic points were found in the absorbance spectra, although crossovers (not isosbestic) were observed in the low pH regime for MECAMS and 3,4-LICAMS. In the derivative spectra, a well-formed isosbestic at 306 nm was observed in the case of 3,4-LICAMS for the high pH buffer region, Figure S9.[52] The Schwarzenbach plot was linear only for a two-proton stoichiometry; the log of the equilibrium constant for this deprotonation was 10.2.

Further analysis of the gallium complex equilibria required non-linear least-squares analysis. Five or six components were obtained for all four metal–ligand systems. The following model, (*6*), worked well for all four titrations.

$$LH_6^{3-} + Ga^{3+} \overset{-3H+}{\longleftrightarrow} GaLH_3^{3-} \overset{-H+}{\longleftrightarrow} GaLH_2^{4-} \overset{-H+}{\longleftrightarrow} GaLH^{5-} \overset{-H+}{\longleftrightarrow} GaL \quad (6)$$

The first deprotonated form of the ligand was included in all cases, but the equilibrium constant for this deprotonation and the absorbance values for LH_5 were fixed to those obtained from the free ligand titration. The equilibrium constants for the hydrolysis of gallium were also included, as non-absorbing species.[53] In summary, the model used for this system included five absorbing species: LH_6, GaL, and three protonated metal–ligand complexes; four parameters were refined: the overall formation constant, β_{110}, and three complex protonation constants, K_{111}, K_{112}, and K_{113}. The five component fit to this model for 3,4-LICAMS is shown in Figure S10.[52]

The refined thermodynamic constants are summarized in Table II; the values obtained potentiometrically, where available, are shown for comparison. The correlations between the calculated protonation constants were low. The Schwarzenbach results indicate that the first two protonations occur simultaneously in the 3,4-LICAMS case and similar results exist for both 3,4-LICAMS and its derivative from potentiometric titrations.

In the cases of 3,4-LICAMS and (DiP)LICAMS, both of the first two protonation constants refined to the same value, 5.8 for 3,4-LICAMS and 6.34 for the alkylated derivative. These protonation constants were correlated at less than 0.50. The species distribution for 3,4-LICAMS, Figure 9, shows the build-up of the mono-protonated intermediate; the MLH species is never present in very high concentration, but it is vital to a good fit of the data. The REFSPEC fit for the Ga–LICAMS data is found in Figure S11.[52] Similar species distributions were obtained for all four Ga–ligand systems. Although the separation between the first and second log A's is much larger for the other two ligands studied, MLH is still not a major component. The build-up of MLH_2 to nearly 100% explains the separation of the two buffer regions observed in all four titrations.

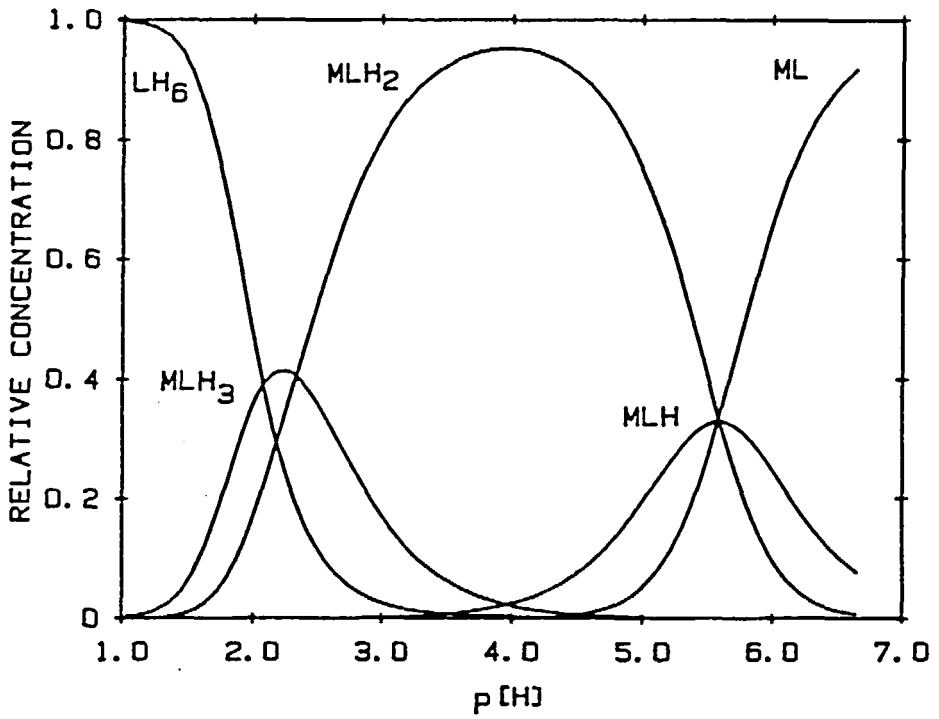

FIGURE 9 Species distribution calculated for the five components in the Ga-LICAMS titration. Metal complexes are normalized to total metal concentration, and ligand-only species to total ligand concentration.

The extinction coefficient spectra of the Ga–MECAMS and Ga–(DiP)LICAMS systems are shown in Figure 10. These represent accurately the properties observed in the raw data: the alkylated derivatives never cross, while the MECAMS spectra are expected to cross over to great extent. It is interesting to compare these spectra with the spectral properties of the Ga–LICAMS system. As in the case of ligand alone, the absorbances are quite broad (Figure 11). The extinction coefficient spectra agree well with the individual spectra for ML, MLH_2, and LH_6. The spectra and second derivative spectra at two different pH values are also shown in Figure 11. The fully formed complex, ML, is the only absorbing species in the high pH spectra, and the doubly-protonated species, MLH_2, dominates the spectra at the lower pH value. The right-hand side shows that, at high pH, the breadth of this absorbance is due to the superposition of three bands, two of which are close together. The doubly protonated species lacks the more separated absorbance and so is sharper. The spectral properties of the five species in solution during the course of these titrations are summarized in Table I.

Kinetics

Addition of gallium to a 10-fold excess of LICAMS in pH 7.4 HEPES buffer yielded a difference spectrum with a large band in the UV, $\lambda_{max} = 348$ nm, $\Delta\varepsilon = 5500\ M^{-1}$

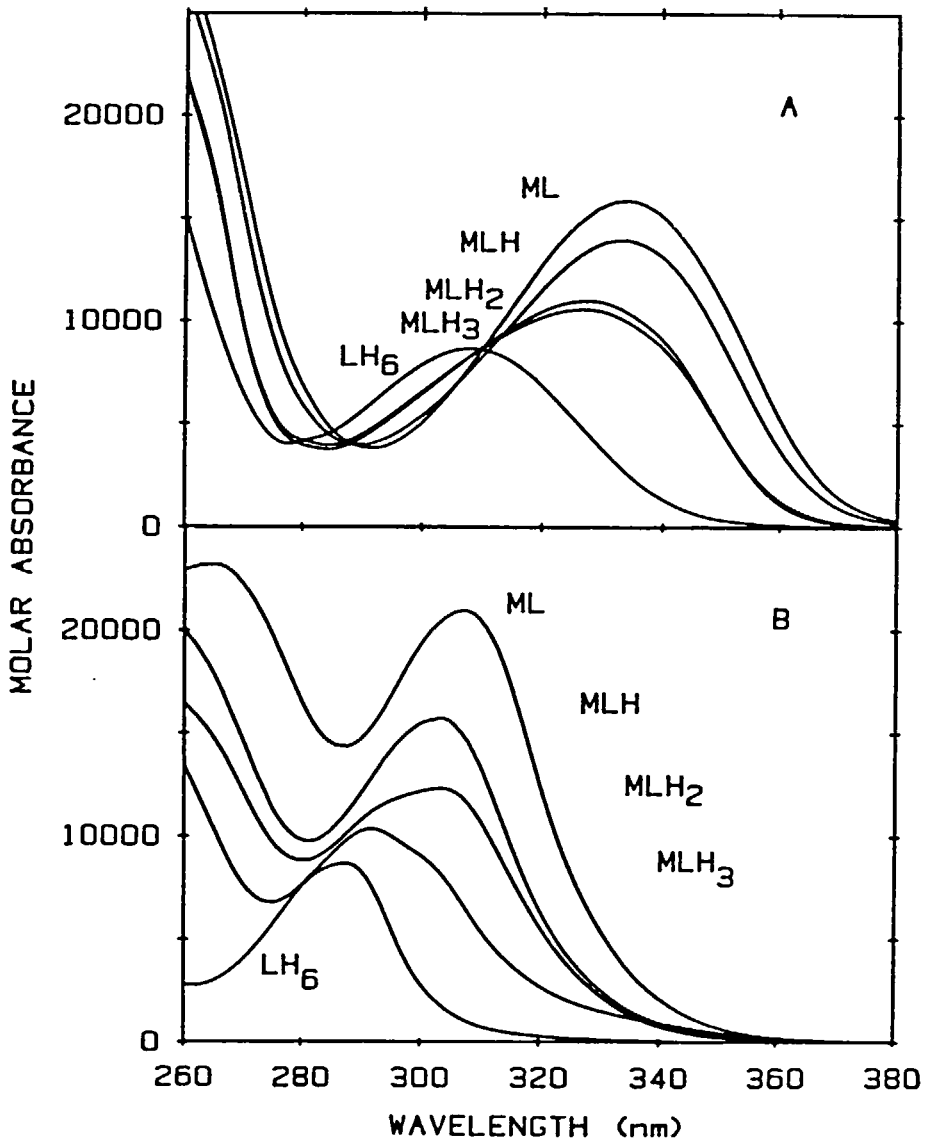

FIGURE 10 Extinction coefficient spectra for the A) gallic–MECAMS and B) gallic–(DiP)LICAMS systems. The latter is representative of the Ga–Me_3MECAMS spectra, as well.

cm^{-1}. This peak was well separated from both the ligand peak at this pH, λ_{max} = 316 nm and the previously described absorbances for apo- and gallic-Tf, λ_{max} = 280 nm.[36] Addition of excess LICAMS to Ga_2-Tf in HEPES buffer at pH 7.4 also resulted in a difference spectrum with λ_{max} = 349 (Figure 12). The noisy region to high energy results from subtracting the absorbance of the ligand, which was in large excess. The absorbance changes as a function of time are replotted in logarithmic form in Figure S12.[52] Decidedly biphasic behaviour was observed, as has been

described for iron removal from Tf.[32,57,58] This phenomenon has been attributed to differences in removal rates between the two protein metal binding sites.[31] The gallium removal data were fitted to one such model, a double-exponential of the form shown in (7).

$$A_{calc} = A_{inf} + (A_o - A_{inf})(c_A e^{-m_1 t} + (1 - c_A)e^{-m_2 t}) \quad (7)$$

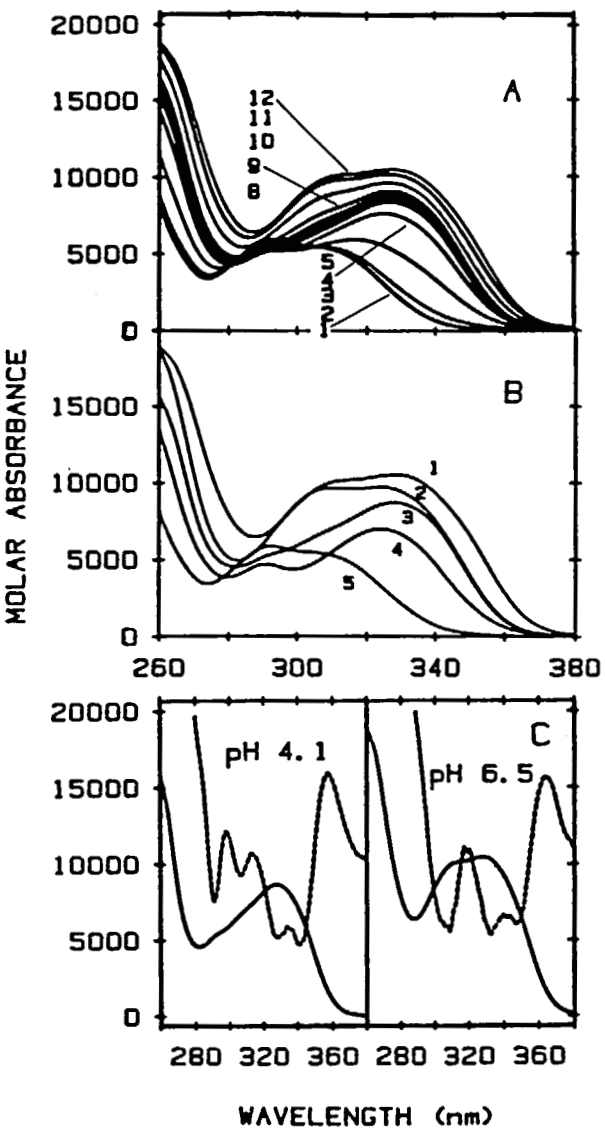

FIGURE 11 Spectroscopic properties of Ga–LICAMS. A) Titration from low to high pH, every 0.5 pH unit shown: 1) pH 1.04, 4) 2.5, 7) 4.01, 10) 5.55, 12) 6.54. B) Extinction coefficient spectra calculated for the five components used in refinement: 1) ML, 2) MLH, 3) MLH_2, 4) MLH_3, 5) LH_6. C) Spectra (-----) and derivative spectra (------) at pH 4.1 (left-hand side) and pH 6.5 (right-hand side) where Ga–H_2LICAMS and Ga–LICAMS, respectively, predominate in solution.

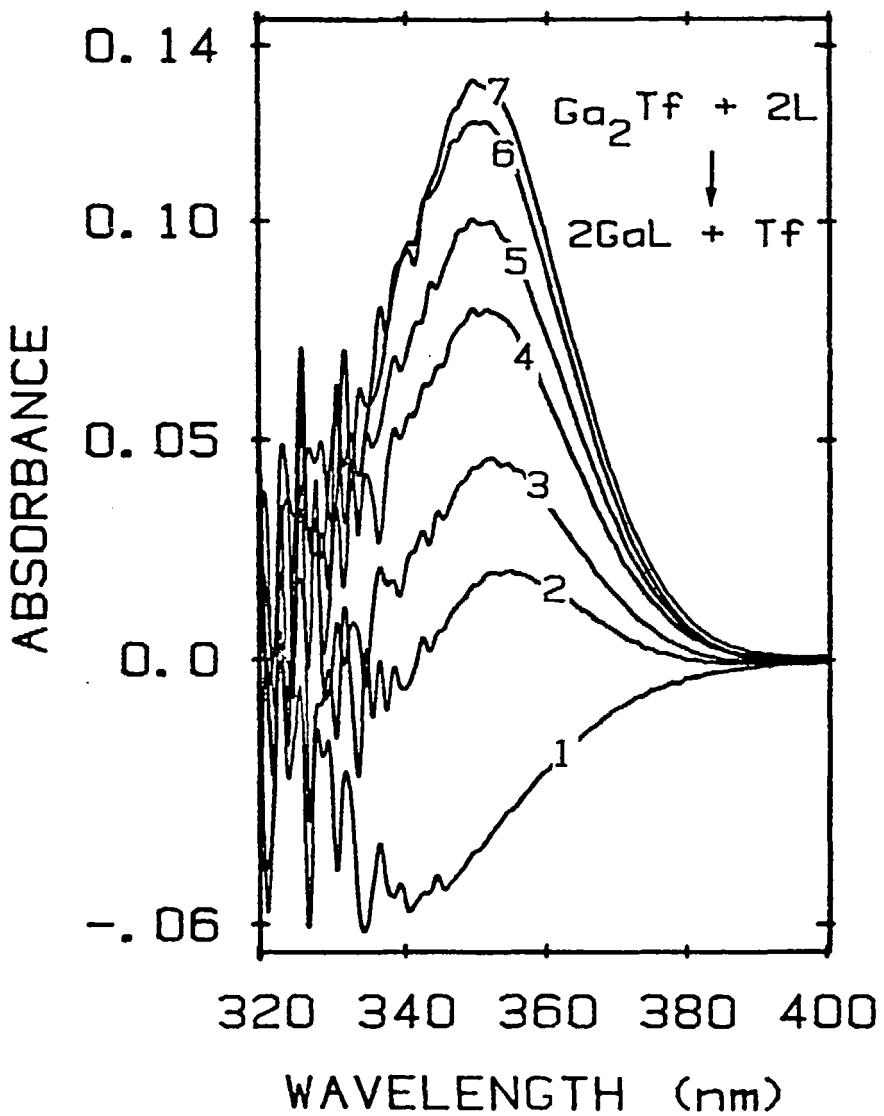

FIGURE 12 Difference UV spectra observed upon addition of excess 3,4-LICAMS (L) to gallic-transferrin (Ga_2Tf), as a function of time. The reaction scheme shown does not include either the proton stoichiometry or the bound bicarbonate anions. Concentrations of reacting species were: 19.3 μM Ga_2Tf, and 580 μM L (15-fold excess over gallium-binding sites); the reference cuvette contained apo-Tf and L at the same respective concentrations. The reaction was run in 50 mM Na/HEPES buffer, pH 7.4 at 25°C. The peak maximum is at 348 nm. Spectra shown are for the following time intervals (t = 0 represents addition of ligand to the sample cuvette, +30 seconds mixing time): *1* (t = 0 min), *2* (t = 1), *3* (t = 2), *4* (t = 5), *5* (t = 10), *6* (t = 60), *7* (t = 300).

The parameters c_A, m_1, and m_2 are all combinations of microscopic rate constants; using the Baldwin notation[31] the assumption is that $k_{1b} = k_{2b}$ and $m_2 \approx m_3$. Then $m_1 = k_{1a} + k_b$, $m_2 = k_b$ and $c_A = 1/2\text{-}1/2\ (m_2/(k_{2a}\text{-}m_1))$. Here m_1 and m_2 are the observed rate constants for metal removal from the faster and slower phases,

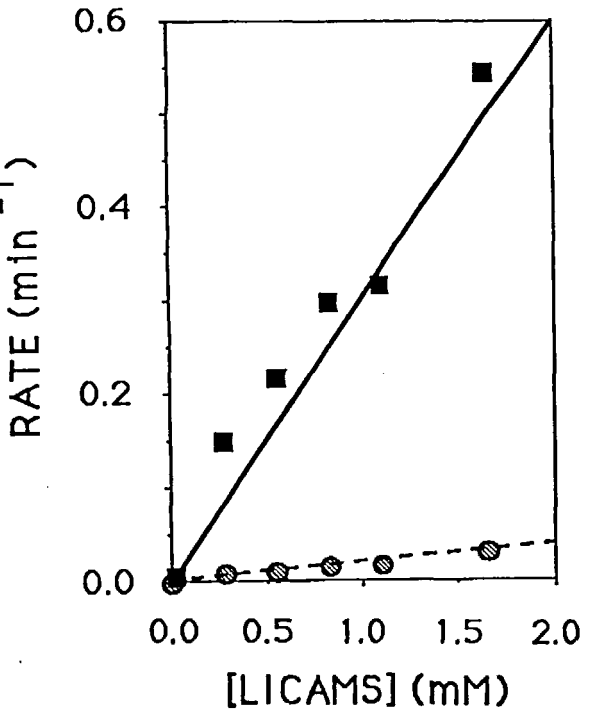

FIGURE 13 Plot of observed macroscopic rate constants m_1 (A) and m_2 (B), as a function of increasing concentrations of 3,4-LICAMS. Experimental conditions are described in Figure 1; $[Ga_2Tf] = 2.75\,\mu M$. The ligand independent rate constants are obtained from the slopes of the lines: $m_1 = 277\,M^{-1}\,min^{-1}$, and $m_2 = 17.0\,M^{-1}\,min^{-1}$.

TABLE III

Summary of the non-linear least-squares analysis of the kinetics of gallium removal from Tf by 3,4-LICAMS; $[Ga_2Tf] = 27.5\,\mu M$ (55.0 μM in metal binding sites). The relative concentration of ligand to gallium sites is shown in column 1. The four parameters varied were A_o, c_A, m_1, and m_2, as described in (7). The latter two are the observed macroscopic rate constants for gallium removal from the two transferrin binding sites. The non-linear least-squares program used, MARQFIT, uses a gradient (steepest descent) method followed by a Taylor-series (Gauss–Newton) method to minimize SSQ, the sum of the squared difference between observed absorbances and calculated values of the parameters.

Ratio of Ligand to Ga3+	No. Data Pts	A_{INF} (Fixed)	Varied Parameters				SSQ
			A_o	c_A	m_1 (sec^{-1})	m_2 (sec^{-1})	
5×	61	0.189	0.076	0.62	2.5×10^{-3}	1.4×10^{-4}	0.89×10^{-4}
10×	72	0.227	0.040	0.65	3.6	1.5	2.47
15×	71	0.213	0.057	0.70	5.0	2.7	1.48
20×	69	0.220	0.062	0.69	5.3	2.7	1.21
30×	53	0.171	0.056	0.78	9.1	5.3	0.83

respectively; c_A represents the apparent amount of metal removed in the first phase the reaction—it approaches 50% as the difference between m_1 and m_2 gets large The fit of the data to theoretically obtained values, (7), was analyzed by nonline least-squares using the basic program MARQFIT.[59,60] Of the five variables, fo were allowed to vary: A_o, c_A, m_1, and m_2. The program generally was unable to refi all five parameters if A_{inf} was allowed to vary also. The initial absorbance, A_o, w not constrained because slight differences in ligand concentration between t reference and sample beam led to relatively large baseline shifts in the differen spectra; changes in A_o compensated for these shifts. A representative fit is shown Figure S13.[52] The results from one complete set of experiments are summarized Table III. The observed macroscopic rate constants, m_1 and m_2, are plotted as function of ligand concentration in Figure 13; the relationship is linear at t concentrations of ligand tested. The second-order rate constants were obtained fro the slopes of the lines ($277\ M^{-1}\ min^{-1}$ and $17.0\ M^{-1}\ min^{-1}$). The correspondi values obtained for iron removal from LICAMS are $24.2\ M^{-1}\ min^{-1}$ a $4.87\ M^{-1}\ min^{-1}$;[32] 3,4-LICAMS is, therefore, at least as kinetically competent removing gallium from Tf as it is at removing iron.

DISCUSSION

Thermodynamic Studies

The comparison between the protonation constants obtained potentiometrically a spectrophotometrically is shown in Table II. The differences for successive proton tion constants (logK) of a given ligand are close to those expected for three no interacting sites; (log 3 is the theoretical minimum difference from statistics). Becau of high correlation between the individual constants for a given ligand, the error the absolute values of the individual constants is much higher than their sums, whi are independent of this correlation and are quite reliable. The average values for 3, LICAMS and MECAMS are essentially identical. The electron-donating charact of an alkyl substituent on the amide of the *N*-alkylated ligands results in protonati constants approximately 0.7 pH unit higher on average than the underivatiz molecules.

For the Ga–CAMS systems, the comparison between the thermodynamic constar obtained potentiometrically and spectrophotometrically is shown in Table II. N value is available potentiometrically for Ga–Me_3MECAMS, but the tris isoprop derivative has log $\beta_{110} = 35$.[21] In all cases, the overall formation constants, β_1 (β_{130} for DMBS), were larger in the spectral determination; up to 3 log un difference was found. This is attributed almost entirely to the new values for t overall formation constants of the ligands themselves (β_{016}). As better values for t first protonation constants (1–3) are now available, these new formation constar should be more accurate than the earlier estimates.[23]

The linear ligands, 3,4-LICAMS and (DiP)LICAMS, have separate one-prot steps which occur at identical pH. The build-up of MLH was very important to t refinement; no model which involved a single two- proton step refined satisfactori The spectra of ML and MLH (Figure 11) are quite similar near 300 nm; neither t Schwarzenbach nor REFSPEC analysis could distinguish between them. The results show the power of using the entire spectrum for analysis. In the low-p regime, the association of the ligand and metal apparently occurs with the initial lc of three protons, yielding MLH_3^{3-}. The complex having a singly bound catech does not appear to be important in the metal-sequestering process.

Spectral Properties

In addition to the thermodynamic differences between the ligands containing secondary and tertiary amides, there were also large spectral differences (Table I). The maxima of the alkylated ligands were shifted 25–30 nm to higher energy compared to the non-alkylated analogues. This may result from electronic stabilization of the ground state (largely carbonyl non-bonding in character), relative to the π^* excited state.

With respect to the mechanism of complexation, the order of protonation of the arms can be extracted from the spectra. In the fully protonated form, the tertiary amides (DMBS, Me_3MECAMS, and (DiP)LICAMS) absorb at ~285 nm (ε of about 3000 per catechol moiety); the fully *ortho*-deprotonated form absorbs at 300 nm (5000 per catechol). The only ligand which contains entirely secondary amides is MECAMS; it absorbs at 310 nm (3000) in the fully protonated form, and at 330 (5000) when triply deprotonated. 3,4-LICAMS, which has one tertiary and two secondary amides, has broad bands with λ_{max} values between those listed above, with lower intensity. The key to the 3,4-LICAMS spectra is the doubly deprotonated LH_4 species. The second derivative spectrum[54–56] shows that this species has a single absorbance maximum, at 327 nm—the same location as MECAMS. The third deprotonation causes a new peak to grow, broadening the absorbance band. In the second derivative, this peak is shown to be at 304 nm, the same location as found for ligands having only tertiary amides. The catechol arm with the tertiary amide—the middle arm—is the last to deprotonate. This is in accordance with the thermodynamic results. That the peak near 330 nm has some fine structure in the second derivative is attributed to the difference between the two arms of the 3,4-LICAMS ligand.

A similar analysis can be carried out on the spectra of the metal complexes. The complexes with DMBS are representative of ligands with tertiary amides; these absorb at about 305 nm with extinction coefficients of 5000–7000 per catechol moiety. Binding of more catechol groups is additive in intensity with only small changes in wavelength. MECAMS, a ligand containing only secondary amides, absorbs at 335 nm with approximately the same intensity per catechol as DMBS. As in the case of ligands alone, 3,4-LICAMS is the key. Ga–H_2LICAMS has a spectrum essentially identical to that of Ga–H_2MECAMS. The second derivative indicates that this comprises just one peak. Upon complete complexation of the metal by 3,4-LICAMS, an addtitional peak appears with its maximum at 308 nm—where the tertiary amides absorb. This indicates that the middle catechol arm is binding last. The spectral changes that occur between the penultimate and final deprotonations are very different—while MLH resembles ML, it is very different from MLH_2. This implies that these protons are removed from dissimilar sites, and also supports the model that the metal binds first to the *ortho* hydroxyl and then adds to the *meta* hydroxyl on the same catechol moiety.

The complexation of gallium by sulfonated catecholamides appears to occur catechol by catechol, in discrete one-proton steps. The following model is proposed for all ligands studied, (*8*),

$$Ga(cat)_2{\cdot}(catH)_2 \longrightarrow Ga(cat)_2(catH) \longrightarrow Ga(cat)_3 \qquad (8)$$

where the $catH_2$ is a free arm in the case of the triscatecholate ligands and completely dissociated ligand for the DMBS monomer. The structural characterization of a

gallium (catH) complex that displays a salicylate mode of bonding[61] supports a model in which the amide carbonyl and *ortho* phenolate coordinate for the catH units. This does not occur for divalent cations such as the Cu^{2+}–MECAMS complex, which has a free, fully-protonated, catecholate arm below pH 5.4;[62] that complex displays an infrared band at 1640 cm^{-1}, corresponding to the free arm.

Kinetics

The large difference between the absorbance maximum of 3,4-LICAMS and Ga–LICAMS makes possible the measurement of small amounts of Ga–LICAMS in the presence of large excesses of the free ligand. The fact that the shift is to low energy is fortuitous, in that proteins such as transferrin typically do not absorb appreciably above 300 nm. At 30-fold excess ligand (about 1.6 mM), the signal-to-noise ratio decreases (from the tail of the LICAMS absorbance into the near UV), so reliable data cannot be obtained from appreciably higher concentrations of ligand. This precluded examining ligand concentrations (3 to 5 mM) where saturation behaviour was seen in Fe^{3+} removal from Tf.[32] The first gallium of Ga_2Tf is removed 12 times faster than the first iron of Fe_2Tf and the ratio between the second order (low ligand concentration) rate constants in the case of gallium is much larger than in the iron case.

Baldwin has proposed the following scheme for release of iron from Tf,

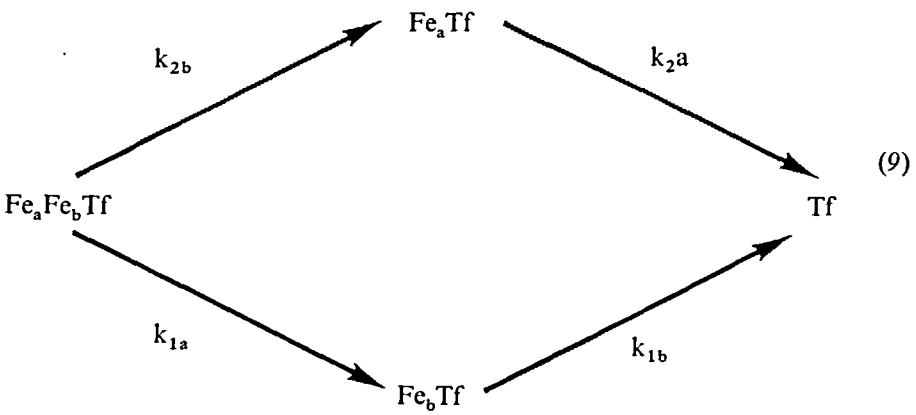

(9)

and has solved the simultaneous rate equations for a series of cases.[57] When the two sites are sufficiently different that $k_{1b} \gg k_{1a}$ (Baldwin's "case 3") then the loss of metal proceeds by only the top pathway (*i.e.* the *N* terminal Ga^{3+} always leaves first in the Ga_2Tf complex) and $c_A = 1/2$. For this simplification to hold, k_{1b} should be $\sim$100 times k_{1a}. If, as found earlier for diferric and monoferric transferrin iron removal by LICAMS,[31] the two rates of removal from the N site are about the same ($k_{1b} = k_{2b}$) then the values of m_1, m_2 and c_A as functions of the microscopic rate constants (described earlier for equation 7) give k_{2a} as a function of the refined parameters c_A, m_1 and m_2 (Table III). The numerical values of k_{2a} thus obtained are consistent with the relative values found in the earlier iron study.[31]

CONCLUSIONS

Catechoylamide-containing ligands are of interest as metal sequestering agents with

potential application in radiopharmaceuticals. This study has used the spectral properties of these ligands to determine thermodynamic and kinetic constants for the complexes they form with the spectrophotometrically inert metal, gallium. Changes in ligand-based transitions have been used to investigate the pathway of complexation of gallium by various catechoylamides and to measure the rates of removal of gallium from transferrin by the hexadentate ligand, 3,4-LICAMS.

Spectrophotometric analysis is a very effective technique for choosing a model for metal complexation by these ligands; far more mechanistic information was obtained by derivative spectroscopy and whole-spectrum analysis than has previously been obtained either by potentiometry or by using simpler spectrophotometric techniques.

Although Ga^{3+} and Fe^{3+} have similar ionic radii and so are both strong Lewis acids, gallium is different from iron in that the former has no low-energy redox couple comparable to that of iron. Hence, in biological studies, gallium is sometimes employed as a non-reducible iron analogue. Although the two metals form structurally similar tris complexes at high pH,[63] they show significant differences in their solution behaviour. The weaker binding of gallium is paralleled by an increase in the rate of removal from Ga_2Tf relative to the diferric complex; the first metal ion removed 12 times as fast and the second 3.4 times as fast relative to Fe_2Tf.

ACKNOWLEDGEMENTS

We are pleased to dedicate this paper to Professor Arthur Martell. This research was supported by NIH grant DK 32999.

SUPPLEMENTARY MATERIAL

Supplementary information, Figures: S1 (Spectral componentization for the DMBS titration using program REFSPEC), S2 (Plot of the calculated fit (solid lines) to each component, as a function of proton concentration, after refinement of the model for the titration of DMBS), Figure S3 (Species distribution predicted from REFSPEC refinement for DMBS, normalized to total ligand concentration), S4 (Extinction coefficient spectrum calculated for the two species in the titration of DMBS), S5 (Spectral titration of Ga–DMBS (0.1 mM Ga, 3-fold excess ligand), from low to high pH), S6 (Spectra titrations of (A) 88.0 μM MECAMS and (B) 70.4 μM Me_3MECAMS from low to high pH), S7 (Calculated fit (solid lines) to spectra components for the four species included in MECAMS model), S8 (Spectrophotometric titrations of (A) MECAMS and (B) Me_3MECAMS, from low to high pH), S9 (First derivative spectra of Ga–LICAMS titration from pH 4.60 to 5.43, every fifth spectrum shown), S10 (The six spectra components obtained in the initial analysis of the Ga–LICAMS titration), S11 (Calculated fits, as a function of proton concentration, to the five components used in analyzing the Ga–LICAMS titration), S12 (Gallium removal from transferrin by 3,4-LICAMS), S13 (Plot of observed macroscopic rate constants m_1 (a) and m_2 (B), as a function of increasing concentrations of 3,4-LICAMS), (16 pages) are available from the senior author.

REFERENCES

1. M.J. Welch and S. Moerlein, ACS Symp. Series. *Inorg. Chem. in Biol. and Med.*, **140**, 121 (1980).

2. P. Hoffer, *J. Nucl. Med.*, **21**, 282 (1980).
3. S.M. Larson, J.S. Rasey, D.R. Allen, N.J. Nelson, Z. Grunbaum, G.D. Harp and D.L. Williams, *J. Nat. Cancer. Inst.*, **64**, 41 (1980).
4. E.N. Baker, S.V. Rumball and B.F. Anderson, *Trends in Biochem. Sci.*, **12**, 350 (1987).
5. P. Aisen and D.C. Harris, *Iron Carriers and Iron Proteins*, T.M. Loehr, Ed., pp. 239–341 (VCH Publishers, New York, 1989); P. Aisen, *ibid*, 353–370.
6. D. Chasteen, *Transferrin, A Perspective. Advances in Inorganic Chemistry*, E.C. Theil, G.L. Eichorn and L.G. Marzili, Eds., pp. 201–234 (Elsevier, New York, 1983).
7. N.-J. Octave, Y.-J. Schneider, A. Trouet and R.C. Crichton, *Tr. Bioch. Sci.*, **8**, 217–220 (1983).
8. H.A. Huebers and C.A. Finch, *Blood*, **64**, 763–767 (1984).
9. A. Ando, I. Ando, T. Hiraki, M. Takeshita and K. Hisada, *Int. J. Nucl. Med. Biol.*, **10**, 1 (1983).
10. A. Ando, I. Ando, T. Hiraki, K. Hisada, K. Nitta and H. Ogawa, *Eur. J. Nucl. Med.*, **9**, 300 (1984).
11. M. Tsan, *J. Nucl. Med.*, **26**, 88 (1985).
12. H. Langhammer, G. Glaubitt, S.F. Hampe, U. Haubold, G. Hor, A. Kaul, P. Koeppe, J. Koppenhagen, H.D. Roedler and J.B. van der Schoot, *J. Nucl. Med.*, **13**, 25 (1972).
13. P.A.G. Hammersley, *Eur. J. Nucl. Med.*, **9**, 467 (1984).
14. Z.H. Oster, S.M. Larson and H.N. Wagner, *J. Nucl. Med.*, **17**, 356 (1976).
15. S.J. Rodgers and K.N. Raymond, *J. Med. Chem.*, **26**, 439 (1983).
16. K.N. Raymond and T.P. Tufano, *The Biological Chemistry of Iron*, H.B. Dunford Ed., pp. 85–105 (D. Reidel Publishing Co., Amsterdam, 1982).
17. K.N. Raymond, W.R. Harris, C.J. Carrano and F.L. Weitl, *ACS Symp. Ser.*, **140**, 314 (1980).
18. B.F. Matzanke, G. Müller-Matzanke and K.N. Raymond, *Iron Carriers and Iron Proteins*, T.M. Loehr, Ed., pp. 1–121 (VCH Publishers, New York, 1989).
19. S.M. Moerlein, M.J. Welch and K.N. Raymond, *J. Nucl. Med.*, **23**, 501 (1982).
20. S.M. Moerlein, M.J. Welch, K.N. Raymond and F.L. Weitl, *J. Nucl. Med.*, **22**, 710 (1981).
21. M.J. Kappel, V.L. Pecoraro and K.N. Raymond, *Inorg. Chem.*, **24**, 2447 (1985).
22. V.L. Pecoraro, G.B. Wong and K.N. Raymond, *Inorg. Chem.*, **21**, 2209 (1982).
23. M.J. Kappel and K.N. Raymond, *Inorg. Chem.*, 3437 (1982).
24. K.N. Raymond, G. Müller and B.F. Matzanke, *Topics in Current Chemistry* **123**, (1984).
25. W.R. Harris, F.L. Weitl and K.N. Raymond, *J. Am. Chem. Soc.*, **103**, 2667 (1981).
26. M.E. Cass, T.M. Garrett and K.N. Raymond, *J. Am. Chem. Soc.*, **111**, 1677 (1989).
27. V.L. Pecoraro, W.R. Harris, G.B. Wong, C.J. Carrano and K.N. Raymond, *J. Am. Chem. Soc.*, **105**, 4623 (1983).
28. S.A. Kretchmar, M. Teixeira, B.-H. Huynh and K.N. Raymond, *Biology of Metals*, **1**, 26 (1988).
29. D.C. Harris, *Biochem.*, **16**, 560 (1977).
30. J. Zweier, P. Aisen, J. Peisach and W.B. Mims, *J. Biol. Chem.*, **254**, 3512 (1979).
31. S.A. Kretchmar and K.N. Raymond, *Biology of Metals*, **2**, 65 (1989).
32. S.A. Kretchmar and K.N. Raymond, *J. Am. Chem. Soc.*, **108**, 6212 (1986).
33. P. Aisen, A. Leibman and J. Zweier, *J. Biol. Chem.*, **253**, 930 (1978).
34. E.H. Morgan, *Biochim. Biophys. Acta*, **580**, 312 (1979).
35. K.N. Raymond, T.D.Y. Chung, V.L. Pecoraro and C.J. Carrano, *The Biochemistry and Physiology of Iron*, P. Saltman and J. Hegenauer, Eds., pp. 650–661 (Elsevier, New York, 1982).
36. W.R. Harris and V.L. Pecoraro, *Biochem.*, **22**, 292 (1983).
37. C.F. Baes and R.E. Mesmer, *The Hydrolysis of Cations* (Wiley, New York, 1976).
38. R.E. Cowart, N. Kojima and G.W. Bates, *J. Biol. Chem.*, **257**, 7560 (1982).
39. S.A. Kretchmar and K.N. Raymond, *Inorg. Chem.*, **27**, 1436 (1988).
40. F.J. Welcher, *The Analytical Uses of Ethylenediamine Tetraacetic Acid (D. van Nostrand Co., Inc., Princeton, New Jersey, 1958).*
41. *F.L. Weitl and K.N. Raymond, J. Org. Chem.*, **46**, 5234 (1981).
42. V.L. Pecoraro, F.L. Weitl and K.N. Raymond, *J. Am. Chem. Soc.*, **103**, 5133 (1981).
43. F.L. Weitl, W.R. Harris and K.N. Raymond, *J. Med. Chem.*, **22**, 1281 (1979).
44. Hewlett-Packard, *8450A UV/Vis Spectophotometer Operators Manual*, Publ. No. 08450-90017 (1981).
45. D. Chasteen, *Coord. Chem. Rev.*, **22**, (1977).
46. C.J. Carrano and K.N. Raymond, *J. Am Chem. Soc.*, **101**, 5401 (1979).
47. T.M. Loomis, *The Coordination Chemistry of Ferric Catecholates*, Ph.D. thesis, University of California, Berkeley (1988).
48. G. Anderegg, F. L'Eplattenier and G. Schwarzenbach, *Helv. Chim. Acta*, **46**, 1400 (1963).
49. R.C. Scarrow, P.E. Riley, K. Abu-Dari, D.L. White and K.N. Raymond, *Inorg. Chem.*, **24**, 954 (1985).
50. P.N. Turowski, S.J. Rodgers, R.C. Scarrow and K.N. Raymond, *Inorg. Chem.*, **27**, 474 (1988).

51. A.J. Waring, *Anal. Chim. Acta*, **153**, 213 (1983).
52. See the last paragraph of this paper regarding supplementary data. Copies of these data are available upon request to the senior author.
53. R.M. Smith and A.E. Martell, *Critical Stability Constants. Vol 4: Inorganic Complexes* (Plenum Press, New York, 1976).
54. A.H. Lawrence, *Tr. Analyt. Chem.*, **2**, V–IX (1983).
55. T.C. O'Haver, *Analyt. Chem.*, **51**, 91A–100A (1979).
56. G. Talsky, L. Mayring and H. Kreuzer, *Angew. Chem. Int. Ed. Engl.*, **17**, 785 (1978).
57. D.A. Baldwin, *Biochim. Biophys. Acta*, **623**, 183 (1980).
58. W.R. Harris, *J. Inorg. Biochem.*, **21**, 263 (1984).
59. G.A. Sagnella, *Tr. Bioch. Sci.*, **10**, 100 (1985).
60. W. Schreiner, M. Kramer, S. Krischer and Y. Langsam, *PC Tech. J.*, **3**, 170 (1985).
61. E. Hahn and K.N. Raymond, to be submitted.
62. M.J. Kappel, *Inorg. Chem.*, **21**, 3437 (1982).
63. B.A. Borgias, S.J. Barclay and K.N. Raymond, *J. Coord. Chem.*, **15**, 109 (1986).